

A Numerical Study of Thickness Effect of the Symmetric NACA 4-Digit Airfoils on Self Starting Capability of a 1kW H-Type Vertical Axis Wind Turbine

Chi-Cong Nguyen, Thi-Hong-Hieu Le, Phat-Tai Tran

Department of Aerospace Engineering, Ho Chi Minh City University of Technology, Ho Chi Minh City, Vietnam

Email address:

nccong@hcmut.edu.vn (C. C. Nguyen), honghieu.le@hcmut.edu.vn (T. H. H. Le)

To cite this article:

Chi-Cong Nguyen, Thi-Hong-Hieu Le, Phat-Tai Tran. A Numerical Study of Thickness Effect of the Symmetric NACA 4-Digit Airfoils on Self Starting Capability of a 1kW H-Type Vertical Axis Wind Turbine. *International Journal of Mechanical Engineering and Applications*. Special Issue: Transportation Engineering Technology — part II. Vol. 3, No. 3-1, 2015, pp. 7-16. doi: 10.11648/j.ijmea.s.2015030301.12

Abstract: The effect of thickness of the symmetric NACA 4-digit airfoil series on self starting of a 1kW three blades H-type vertical axis wind turbine (VAWT) using computational fluid dynamic (CFD) analysis is the main objective of this study. A sliding interface technique was used to investigate two dimensional unsteady flow around VAWT model by solving the Reynolds Average Navier-Stokes equation with k-ε Realizable turbulent model. A novel CFD-dynamic coupling model is proposed to solve the dynamic of VAWT. In this model, while the aerodynamic force acting on the VAWT blades is solved by CFD, the torque of the generator and the dynamic friction force at the bearing applying on the axis of VAWT are modelled via their physical characteristics. The during time to rotate an angle of 120° of VAWT is one of the principle parameters to investigate the self starting capability. The effect of the starting azimuth angle of blade, the wind velocity and the geometry of the airfoil (NACA 0012, 0015, 0018, 0021) on self starting capability are analysed. The qualitative result show that the considered VAWT has the highest self starting capability when the starting azimuth angle of blade is in the range of [90°÷100°] and it has the lowest self starting capability when the starting azimuth angle is in the range of [45°÷60°]. By using the CFD-dynamic coupling model and by comparing the aerodynamic moment of the wind on the steady three blades to the static friction moment, the considered VAWT rotate at the starting wind velocity of 4 m/s, 3.5 m/s, 3m/s and 3 m/s for NACA 0012, 0015, 0018 and 0021 respectively. The VAWT has the lowest self starting capability with the configuration of NACA 0012 and has the highest capability with NACA 0021.

Keywords: Wind Energy, Wind Turbine, Vertical Axis, Self Starting, CFD, Unsteady Flow, Moving Mesh

1. Introduction

It is noted that the configuration currently exploited around the world are horizontal axis wind turbines. The main reason is that horizontal axis wind turbines offer several advantages over vertical axis wind turbines. Horizontal axis wind turbines give a high efficiency at high tip speed ratio and high self-starting capability. In recent years, there has been a resurgence of interest in vertical axis wind turbines, however. The number of vertical axis wind turbine that have been developed and deployed in the high wind power potential countries and regions over the world has increased considerably. Vertical axis wind turbines offer several other advantages over horizontal axis wind turbines. The simplicity configuration is the main advantage of vertical axis wind turbines. The generator and the gearbox of a vertical axis wind

turbine can be positioned on the ground, therefore reducing the loads on the tower and facilitating the maintenance of the system. In addition, vertical axis turbines do not require a yaw control system because of insensitive to the wind direction capability. The main drawback of vertical axis wind turbine are low self-starting capability and high starting wind speed.

A large number of analytical, numerical, and experimental methods have been used to simulate the flow environment around vertical axis wind turbine. The stream-tube that were proposed by Strickland [1] and Paraschivoiu [2] are the most simple analytical models to investigate the aerodynamic characteristics of vertical axis wind turbine but it does not give enough accuracy for prediction. The most popular stream-tube model is the Double Multiple Stream-tube model (DMST). The

stream-tube models are base on BEM (Blade Element Momentum) models that was first introduced by Glauert [3]. The main drawback of these stream-tube models is that the aerodynamic characteristic of airfoil, the empirical formulas of dynamic stall must be included in the models. The free wave vortex methods that were suggested by Strickland et al. [4] and Coton et al. [5] give more accuracy on performance prediction but require more complexity on numerical point of view.

In recent years, increased availability of high-performance computing allows the aerodynamics of vertical axis wind turbines to be investigated by solving the Navier–Stokes equations. Hansen and Sørensen [6], as well as Ferreira et al. [7] solved the Reynolds Averaged Navier–Stokes equations to investigate a two-dimensional straight-bladed rotor configuration. In this simulation, the cyclic condition was set to simulate just one blade of a vertical-axis wind turbine. Raciti Castelli et al. [8] proposed a new straight-bladed VAWT performance prediction model, also based on Reynolds Average Numerical Simulation, in order to determine the rotor power curve.

Detached-eddy simulations of a vertical axis wind turbine were performed by Horiuchi et al. [9]. Iida et al. [10] realized a large eddy simulation to investigate aerodynamic characteristic and dynamic structures of flow around a straight-bladed vertical axis wind turbine.

Although there were many studies on performance and aerodynamic characteristic of vertical axis wind turbine, the application of numerical methods that has been performed to analyze the self-starting capability of vertical axis wind turbines, to the authors' knowledge, are so few. Dominy et al. [11] used analytical method to investigate the self-starting of vertical axis wind Darrieus turbines using of NACA 0012 airfoil. Beri and Yao [12] performed the Reynolds Average Numerical Simulation to simulate a vertical axis wind turbine using of the wing profile NACA 0018 with flap. By both unsteady and steady simulation through the wind turbine, they proved that the wind turbine using of NACA 0018 airfoil with flap can startup better than with the wind turbine using the wing profile NACA 2415 at low tip speed ratios. In parallel, Beri and Yao [13] also analyze the influence of the wing chamber on the self-starting capability of wind turbine.

The goal of this investigation is to focus on self-starting capability analysis of 1 kW three blades H-type vertical axis wind turbines using the numerical method.

2. Numerical Model and Validation

2.1. Model Geometry

An 1kW three blade H-type vertical axis wind turbine was designed using the analytical method [14]. The considered wind turbine was coupled with a small generator GL-PMG-1000 [15], which has the power versa rpm curve given by the constructor, through a gearbox of 1/3 transmission. The main geometrical features of the model are summarized in Table 1.

Table 1. Main geometrical features of the wind turbine 1kW

Parameters	
Diameter of rotor, D [m]	3
Height of blades, H [m]	3.5
Number of blades, N [-]	3
Airfoil	NACA 0012 NACA 0015 NACA 0018 NACA 0021
Chord, c [m]	0.25
Solidity, $\sigma = Nc/D$ [-]	0.25
Axis position [mm, mm]	(0, 0)
Inertia moment, I_{zz} [kg.m ²]	115

Azimuth coordinate θ of a blade is the angle between the vertical axis and the line drawn from the origin through the center of pressure of the blade. Blade 1 is defined as the smallest azimuth coordinate. A positive rotation is in the anti-clockwise direction as showed in Fig. 1.

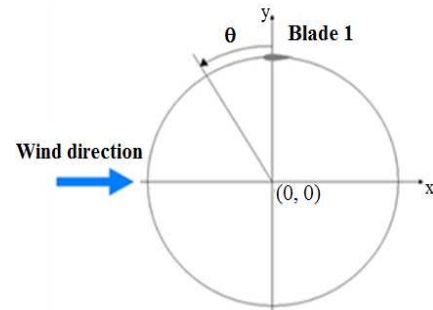


Figure 1. Azimuth coordinate of a blade.

2.2. Spatial Domain Discretization

The template is used to format your paper and style the text. All margins, column widths, line spaces, and text fonts are prescribed; please do not alter them. You may note peculiarities. For example, the head margin in this template measures proportionately more than is customary. This measurement and others are deliberate, using specifications that anticipate your paper as one part of the entire publication, and not as an independent document. Please do not revise any of the current designations.

As the aim of the present work is to reproduce the operation of a rotating wind turbine, the use of moving mesh (sliding mesh) technique is necessary. In particular, the computation domain is divided into two distinct sub-mesh:

- *Wind turbine external*: a rectangular outer fixed zone with a opened circular centered on the turbine rotation axis, using to determine the overall calculation domain.
- *Wind turbine intermediate*: a circular inner moving zone, rotating with rotor angular velocity ω .

The description of two domains are detailed by Raciti Castelli et al. [8] and some technical notes are summarized in the following paragraphs.

2.2.1. Wind Turbine External

In order to allow a full development of the wake generated by the vertical axis wind turbine and to avoid the solid

blockage, the inlet and outlet boundary are positioned respectively 27D upwind and 50D downwind with respect to rotor axis as shown in Fig. 2.

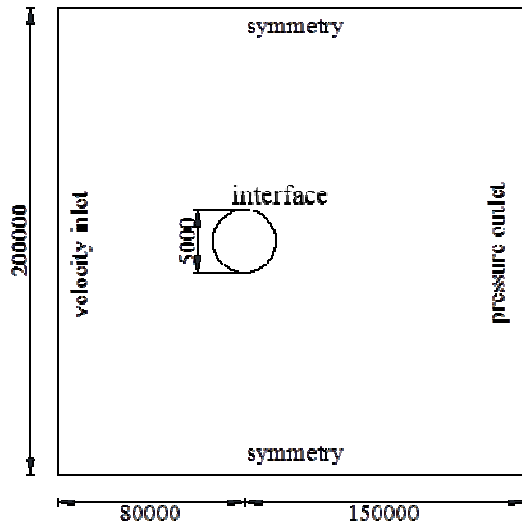


Figure 2. Dimensions of the wind turbine external domain (in mm).

Two side walls are set as symmetry boundary conditions. The circumference around the opened circular centered on the rotation axis is set as interface condition. This interface condition ensure the continuity in the flow field between the *wind turbine external* and the *wind turbine intermediate*.

Fig. 3 shows the unstructured mesh that is chosen for the *wind turbine external* domain.

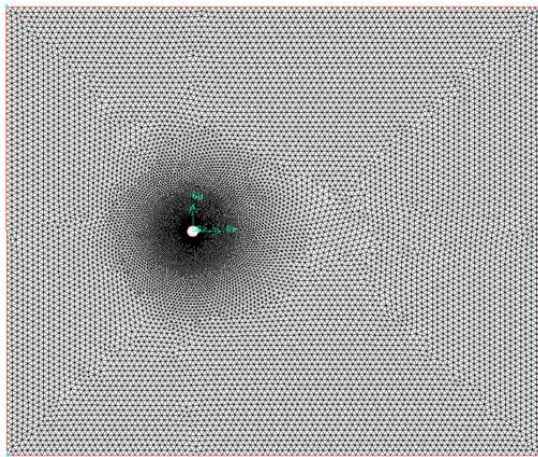


Figure 3. Wind turbine external mesh.

2.2.2. Wind Turbine Intermediate

The *wind turbine intermediate* is modeled as the revolution of the wind turbine and is therefore set as a moving mesh. Thus, the *wind turbine intermediate* rotate at the same angular velocity of the wind turbine. The outer circular of the *wind turbine intermediate* is also set as interface condition. Its location coincides exactly with the interface inside the *wind turbine external* domain.

The main dimensions and the boundary conditions of the wind turbine intermediate domain is shown in Fig. 4.

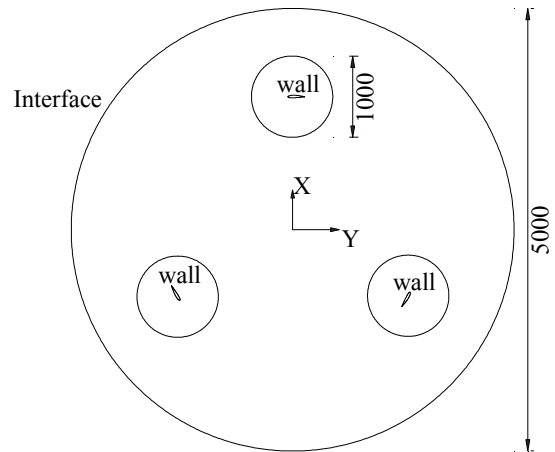


Figure 4. Dimension of the wind turbine intermediate domain (in mm).

To ensure the fast convergence, the mesh on both sides of the interface (*wind turbine external* and *wind turbine intermediate*) is meshed with smooth transition in characteristic size of cells.

To control the smooth evolution of mesh size, all blade profiles inside the *wind turbine intermediate* domain are enclosed in a control circle of 1000 mm diameter and an appropriate size function is adopted.

A growth factor of 1.1 is set for the *wind turbine intermediate*. Therefore the grid size expand from 0.3 mm close to the blade profiles, to 7.5 mm near the control circles and to 25 mm at the interface of the domain, as shown in Fig. 5-7.

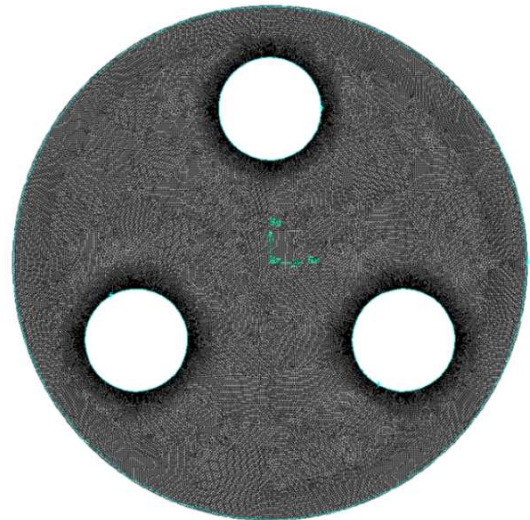


Figure 5. Wind turbine intermediate mesh.

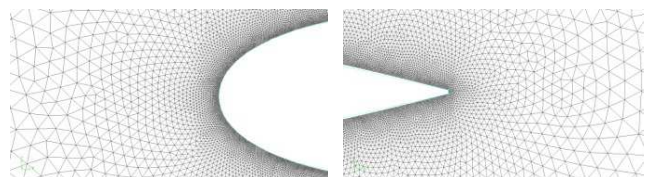


Figure 6. Grid close to leading edge and trailing edge.

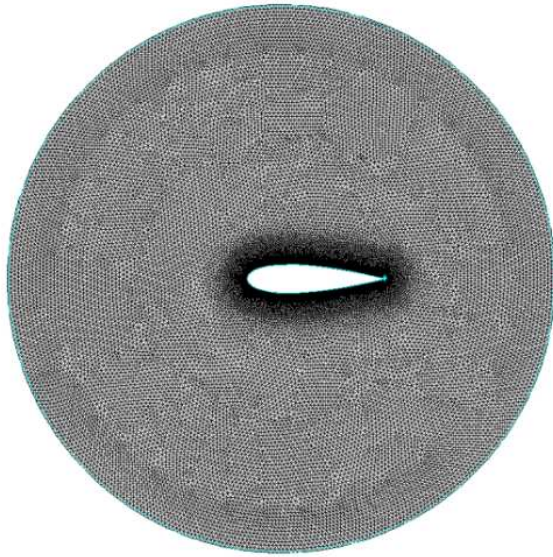


Figure 7. Grid for blade section.

2.3. Validation

In order to investigate the self-starting capability of the 1 kW H-type vertical axis wind turbine, a validation procedure is performed. The similar configuration, as realized by Raciti Castelli *et al.* [8], is chosen. The validation cases are based on H-type vertical axis wind turbine model with constant wind speed at inlet boundary, $V = 9$ m/s. It has the maximum performance at Tip Speed Ratio of 2.33. Eight rotor angular velocity value are imposed on the moving mesh to simulate the revolution of the wind turbine rotor at eight Tip Speed Ratio. The main features of the validation model are summarized in Table 2 [8].

Table 2. Main features of the validation model

Parameters	
Diameter of rotor, D [m]	1.03
Height of blades, H [m]	1
Number of blades, N [-]	3
Airfoil	NACA 0021
Chord, c [m]	0.858
Solidity, $\sigma = Nc/D$ [-]	0.25
Axis position [mm, mm]	(0, 0)
Wind velocity, V [m/s]	9
Tip Speed Ratio-TSR, $\lambda = \omega D/2V$	2.33
Rotor angular velocity, ω [rad/s]	40.718
Reynolds number	300000

It is noted that the aerodynamic analysis based on the numerical model, proposed by Raciti Castelli *et al.* [8], is well valid to the experimental results. Therefore, the numerical scheme is chosen similar to the scheme proposed by Raciti

Castelli *et al.* [8]. In order to simulate the flow environment over the wind turbine, the Reynolds Average Navier-Stokes equations using k- ϵ Realizable turbulence model are solved. To take into account the boundary layer effect at three blade profiles, the characteristic of mesh with y-plus value around 1 is generated. Thus, the Enhanced Wall Treatment configuration is set to three blades profiles. Turbulent intensity and turbulent viscosity ratio are set respectively 0.1% and 1 for all boundary conditions and initial condition. The coupling pressure-velocity solver is based on the SIMPLEC algorithm.

The comparison of actual numerical results with those realized by Raciti Castelli *et al.* [8] are shown in Fig. 8, Fig. 9 and Fig.10. The comparisons show that the numerical model can reproduce most of main features of distribution of moment coefficient, distribution of power coefficient and average power coefficient as shown respectively in Fig. 8, Fig. 9 and Fig. 10. The instantaneous moment coefficient $C_T(\theta)$ and the instantaneous power coefficient $C_p(\theta)$ are defined respectively as:

$$C_T(\theta) = \frac{T(\theta)}{1/2\rho A_s R V^2} \tag{1}$$

$$C_p(\theta) = \frac{P(\theta)}{1/2\rho A_s R V^3} \tag{2}$$

in which, T is aerodynamic torque of rotor, P is power generated by aerodynamic force on blade, ρ is density of air and A_s is rotor swept area.

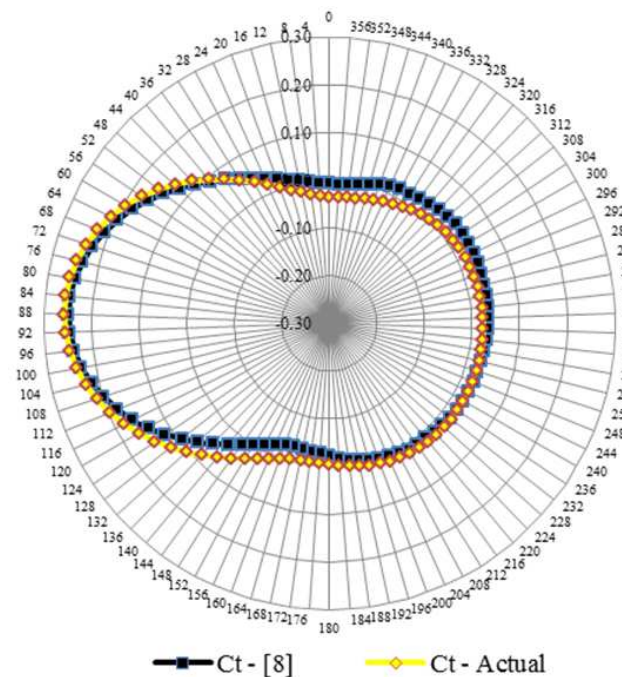


Figure 8. Distribution of moment coefficients in function of azimuth position for blade 1 at TSR = 2.33.

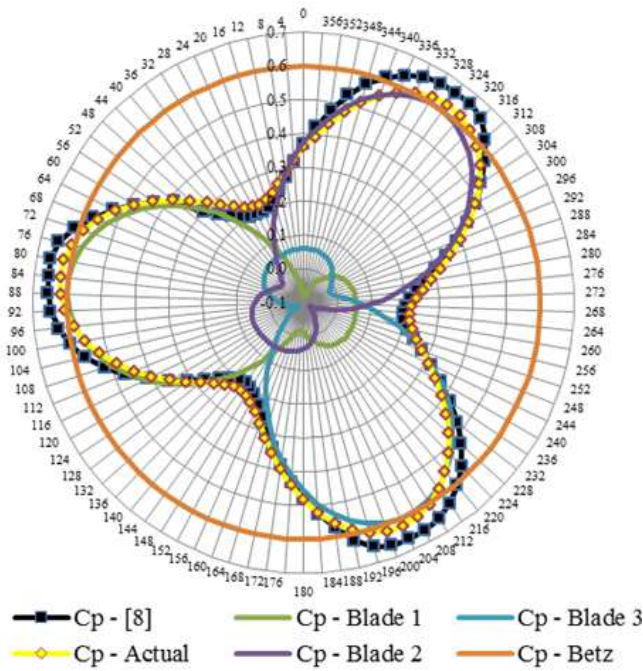


Figure 9. Distribution of power coefficients in function of azimuth position at TSR = 2.33.

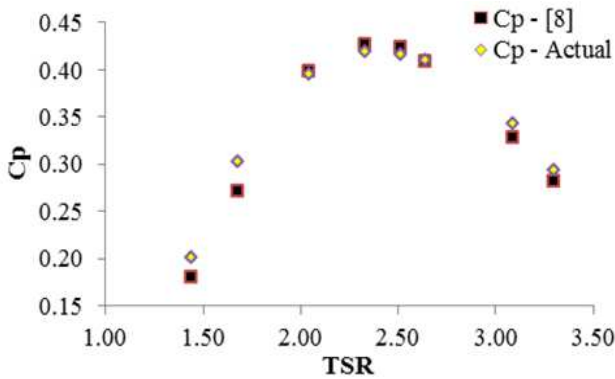


Figure 10. Average power coefficients in function of Tip Speed Ratio.

The distribution of moment coefficients in function of azimuth coordinate for blade 1 at Tip Speed Ratio of 2.33, show that the positive moment coefficients appear when the blade 1 revolves from 0° to 180° of azimuth position. The highest moment coefficient is at azimuth position of 90°. On the other hand, the moment coefficients are very low from 180° to 360° of azimuth coordinate.

The power coefficient can be inferred from moment coefficient. shows that although there is a light difference in power coefficient at maximum and minimum regions between actual result and that presented by Raciti Castelli et al. [8], the distribution of power coefficient is well estimated by actual numerical model. As shown in, one cycle of power coefficient in function of azimuth position is 120°.

The performance of wind turbine, the average power coefficient in function of Tip Speed Ratio, can be reproduced in Fig. 10. The most efficiency performance of wind turbine is at Tip Speed Ratio of 2.33.

These validations show that the actual numerical model can

be applied to analyze the self-starting capability of the designed 1kW H-type vertical axis wind turbine.

3. Self-Starting Analysis

3.1. Revolution time analysis

The goal of this paragraph is to present a new methodology to study the self-starting capability of wind turbine. The revolution time is one of most important parameter to evaluate a wind turbine system (including wind turbine coupling with its generator and bearing) that can be considered as fast, low or no starting capability under a wind velocity. For a three blades wind turbine, the revolution time is the during time that the wind turbine takes to revolute 120° about its axis from the starting azimuth position. To obtain the revolution time parameter of wind turbine, the dynamic equation of wind turbine, as shown in the following formulation, is solved using a coupling CFD-dynamic process:

$$I_{zz} \dot{\omega} = T_{wind} - T_g - T_f \tag{3}$$

in which I_{zz} , T_{wind} , T_g , T_f are inertia moment of wind turbine, torque of wind acting on blades, torque of generator and torque of dynamic bearing friction acting on axis of wind turbine respectively.

In this coupling CFD-dynamic process, while the wind torque that acting on blades of wind turbine is simulated by numerical model solver, friction torque on bearing and generator torque are modeled. From the specification of generator, it is possible to model the generator torque curve as a function of revolution speed as shown in (4). On the other hand the friction torque on bearing is modeled by (5) as defined in [16], [17]:

$$T_g = \frac{1}{2} \rho A_s R^3 \frac{C_{pmax}}{\lambda_{opt}^3} [\omega(t)]^2 \frac{\omega(t)}{|\omega(t)|} \tag{4}$$

$$T_f = f_r \omega(t) \tag{5}$$

Then dynamic equation of wind turbine is solved by first order Euler scheme to find position and angular velocity at next time step of simulation. This process will be repeated until the turbine startup as shown in Fig. 11.

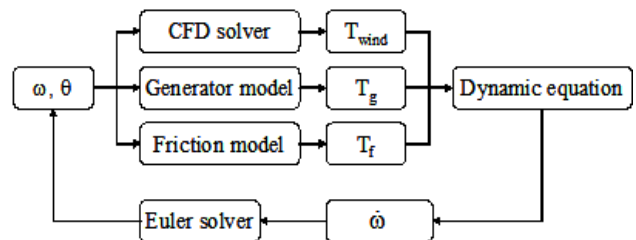


Figure 11. Self-starting analysis diagram.

This new coupling CFD-dynamic combined effects of external factors such as friction moment, generator moment and influence of tracks back flow from the front blade to the

rear blade during operation of wind turbine rotor.

3.2. Starting wind speed determination

Starting wind speed is defined as the lowest wind speed at which the wind turbine has self-starting capability and obtain a revolution of 120° after a finite *revolution time* with any starting azimuth position of blade 1. Static friction moment ($T_{friction-s}$) is normally higher than dynamic friction moment, thus to find out the *starting wind speed* of one wind turbine, it is necessary to follow the steps.

Step 1: analyzing startup characteristic, *revolution time*, of turbine at various starting azimuth position and evaluating its starting azimuth position of blade 1 which make the wind turbine to be dynamically the lowest self-starting capability.

Step 2: the flow through the turbine is simulated in static condition, without rotation, to determine a wind speed that can create wind moment greater than static friction moment.

Step 3: when the turbine could move, the wind moment at this wind speed will be further compared with sliding friction moment and generator moment in rotation condition by using the coupling CFD-dynamic simulation [cf. 3.1]. If wind speed cannot be verified, then select another greater wind speed.

Step 4: starting wind speed is the lowest wind speed that satisfies any hard startup azimuth.

This procedure can be resumed in Fig. 12.

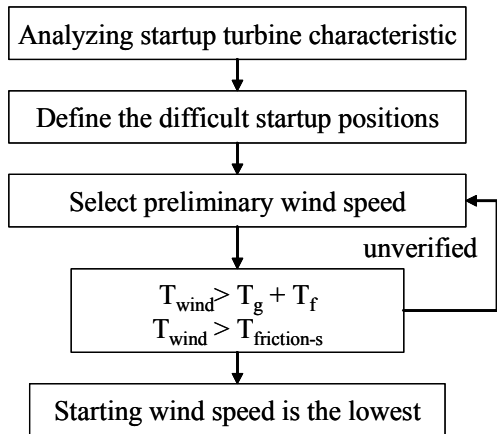


Figure 12. Starting wind speed determination diagram.

4. Results and Analysis

4.1. Self-Starting Characteristics

Supposing that the wind moment is higher than the static friction moment ($T_{wind} > T_{friction-s}$). Fig. 13 shows the *revolution time* or startup time of H-type vertical axis wind turbine 1 kW corresponding to various starting azimuth positions ($0^\circ < \theta < 120^\circ$), three wind speed of 3 m/s, 5 m/s, 7 m/s and four symmetric NACA 4-digit airfoils: NACA 0012, NACA 0015, NACA 0018, NACA 0021.

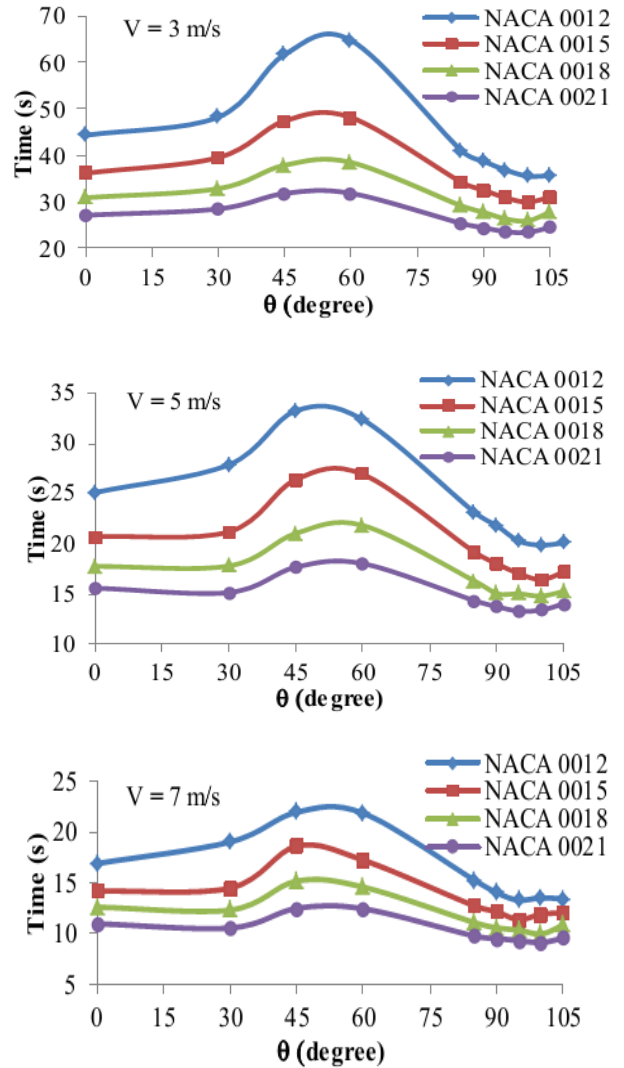


Figure 13. Revolution time in function of starting azimuth position of blade 1.

Fig. 13 shows that for starting azimuth position $\theta = [45^\circ, 60^\circ]$ the turbine has the longest startup time, followed by $\theta = [0^\circ, 30^\circ]$, and has the fastest startup time for $\theta = [90^\circ, 100^\circ]$. The starting azimuth region, $\theta = [45^\circ, 60^\circ]$, is the hardest azimuth position for any airfoils considered in this study. Thus, the considered H-type VAWT has the highest self-starting capability when the starting azimuth angle of blade 1 is in the range of $[90^\circ \div 100^\circ]$ and it has the lowest self-starting capability when the starting azimuth angle is in the range of $[45^\circ \div 60^\circ]$.

Startup time of the wind turbine is also better when the wind speed or thickness airfoils are increased.

- *Starting azimuth position*

To find out the influence of starting azimuth position on revolution time or startup time, the evolution of angular velocity of the turbine in function of azimuth position from different starting azimuth position is investigated for NACA 0021 airfoil and wind speed at 3 m/s as shown in Fig. 14.

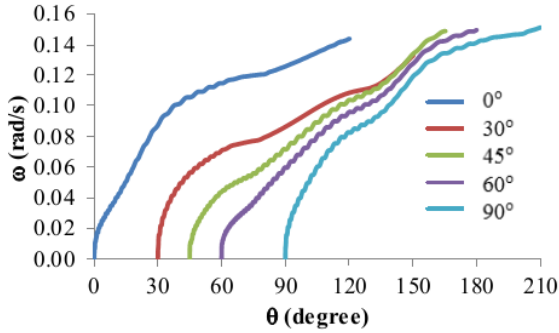


Figure 14. Evolution of angular velocity, NACA 0021, $V = 3$ m/s.

It is noted that when the moment coefficient of three blades are superposed, in the cycle of well operation, the turbine has region of low moment [cf. 0], this is azimuth position of $\theta = [45^\circ, 60^\circ]$. Thus, starting azimuth position if affected in the region of $\theta = [45^\circ, 60^\circ]$ will take a longer startup time than in the region of $\theta = [0^\circ, 30^\circ]$. Furthermore, if starting azimuth position is effected within the region of $\theta = [90^\circ, 100^\circ]$ with the biggest moment, the angular velocity of the turbine will be accelerated fast and the best startup time is obtained.

So the considered H-type vertical axis wind turbine has the shortest startup time in the starting azimuth position around $\theta = [90^\circ, 100^\circ]$ and longest startup time in the region of $\theta = [45^\circ, 60^\circ]$.

• Velocity

Analyzing NACA 0015 airfoil, Fig. 15 shows that increasing wind velocity make turbine tend to startup more quickly.

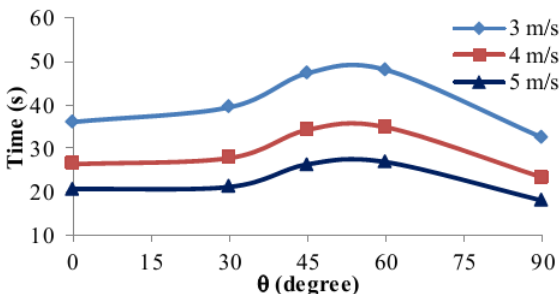


Figure 15. Startup time at different start position and wind speeds, NACA 0015 airfoil.

It is noted that during the startup procedure, the total moment of three blades is highly correlated to the moment affected on blade 1 as shown later on Fig. 16 and Fig. 17. Looking the variation of the moment coefficient of blade 1 with different velocities, at the same starting azimuth position condition, $\theta = 0^\circ$, and for particular NACA 0015 airfoil, as shown in Fig. 16, is the simplest way to investigate effect of wind velocity on startup time. Note that the moment contribute to start up process nearly constant in function of wind velocity when blade 1 has the azimuth position of $[45^\circ, 120^\circ]$. The main difference in magnitude of the maximum moment coefficient on blade 1 can be observed when the azimuth position of blade 1 is $[0^\circ, 45^\circ]$.

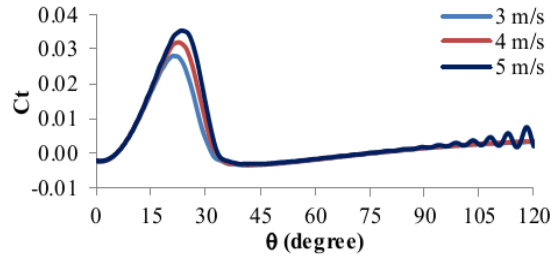


Figure 16. Moment coefficient in blade 1, NACA 0015 airfoil.

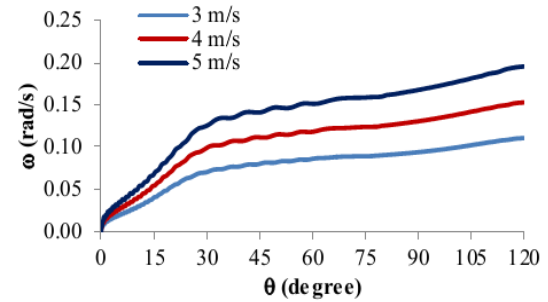


Figure 17. Angular velocity ω from start position $\theta = 0^\circ$ to the completion of the rotation angle of 120° , NACA 0015 airfoil.

Fig. 17 showed the evolution of angular velocity of wind turbine with NACA 0015 in startup process at the starting azimuth position of $\theta = 0^\circ$ and with different wind velocity. It is noted that the difference in rate of change of angular velocity in the region of $[0^\circ, 45^\circ]$ is observed which is highly correlated to the variation of maximum moment coefficient in function of wind velocity as shown in Fig. 16. On the other hand, the similar rate of change of angular velocity of wind turbine is also noted when blade 1 has the azimuth position of $[45^\circ, 120^\circ]$ which is correspondent to the no variation in moment coefficient in function of wind velocity.

• Airfoil thickness

Similar to the analysis of effect of velocity and starting azimuth position, Fig. 13 shows that startup time is smaller for larger thickness.

To consider the impact of airfoil, Fig. 18 presents the effect of different thickness NACA airfoil on moment coefficient of blade 1 with the starting position of $\theta = 0^\circ$.

Fig. 13 shows that the airfoil with higher thickness makes the region of maximum moment coefficient which contributes to the startup process increase both in larger and in magnitude. Therefore, the larger thickness airfoil the higher self-starting capability is obtained.

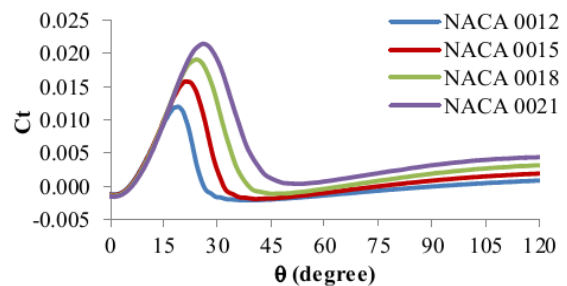


Figure 18. Moment coefficient in blade 1, starting azimuth position of $\theta = 0^\circ$.

4.2. Starting Wind Speed

To take into account the starting wind speed determination diagram, the flow over the static wind turbine with the azimuth position of $\theta = 45^\circ, 60^\circ$ and 75° , which is the region of lowest self-starting capability, is simulated.

Fig. 19, Fig. 20, Fig. 21 and Fig. 22 show the wind moments and the static friction moments at their minimum wind speeds that make the wind moments greater than the static friction moments in static condition. On the other hand, the H-type wind turbine cannot move or cannot startup at a lower wind speed presented in Fig. 23. The variation of wind moments is due to influence of wake detached at back flow of wind turbine or the separation of boundary layer in blade.

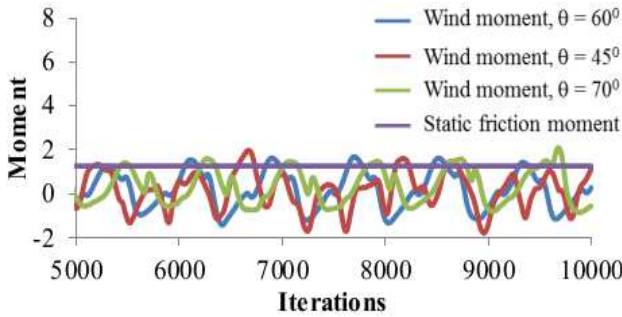


Figure 19. Wind moment and static friction moment at $V = 4$ m/s, NACA 0012.

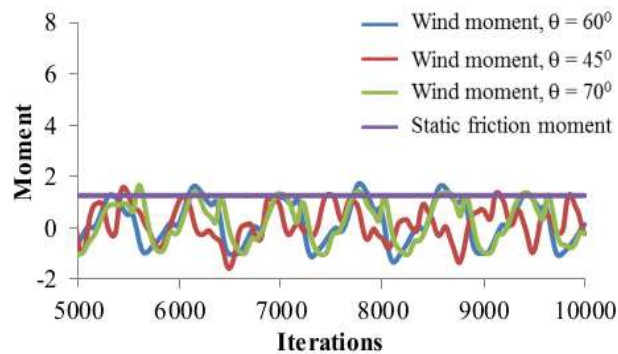


Figure 20. Wind moment and static friction moment at $V = 3.5$ m/s, NACA 0015.

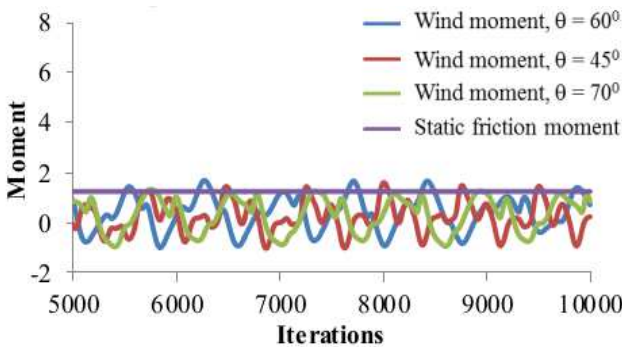


Figure 21. Wind moment and static friction moment at $V = 3$ m/s, NACA 0018.

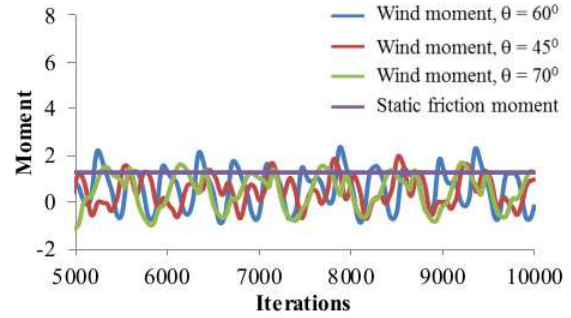


Figure 22. Wind moment and static friction moment at $V = 3$ m/s, NACA 0021

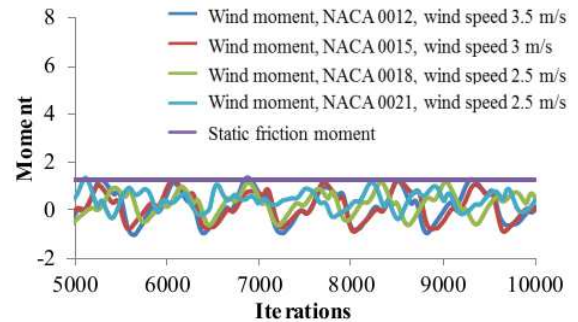


Figure 23. Wind moment and static friction moment at no startup wind speed, starting azimuth position of $\theta = 60^\circ$.

In the self-starting characteristics of the turbine [cf. 4.1] shows that wind speeds being greater than 3 m/s can reproduce the wind moment that overcome sliding friction moment and generator moment. Thus, it is considered that the starting wind speeds are the lowest wind speeds made turbine change from static condition to dynamic condition as summarized in Table 3.

Table 3. Starting wind speeds

Airfoils	Starting wind speeds (m/s)
NACA 0012	4.0
NACA 0015	3.5
NACA 0018	3.0
NACA 0021	3.0

5. Conclusions

This study presents a coupling between CFD model and dynamic model of the wind turbine motion. To the authors' knowledge, this coupling is a new method in the analysis of self-starting capability of vertical axis wind turbine. A novel procedure to determine the starting wind speed is also proposed.

There are three factors affecting on the self starting capability of the 1 kW H-type vertical axis wind turbine such as starting azimuth position, wind speed, wing profile. Starting azimuth position is the main factor effects. High effect of airfoil thickness on startup time of the wind turbine is highly recommended. The lowest wind speed turbine, that make the wind turbine to be self starting at every starting azimuth position corresponding to each type wing profile, is determined.

The considered 1 kW H-type vertical axis wind turbine can

start up well with NACA 0021 airfoil. This turbine possesses the high self-starting capability at the starting azimuth position of $\theta = [90^\circ, 100^\circ]$.

The results from this analysis method can be used to analyze for all turbines with different airfoils and database for higher research on vertical axis wind turbines.

Acknowledgements

The authors would like thank to the Research Fund of Ho Chi Minh City University of Technology for its financial support to the research project T-KTGT-2014-41.

References

- [1] J. H. Strickland, "The Darrieus Turbine: A Performance Prediction Model Using Multiple Streamtubes", Sandia National Labs, Rept. SAND75-0431, Albuquerque, NM, 1975.
- [2] I. Paraschivoiu, "Double-Multiple Streamtube Model for Studying Vertical-Axis Wind Turbines", *Journal of Propulsion and Power*, Vol. 4, 1988, pp. 370–377.
- [3] H. Glauert, "Airplane propellers", *Aerodynamic Theory*, vol. 4. New York: Dover Publication Inc, 1963. Division L, pp. 169-360.
- [4] J. H. Strickland, B. T. Webster, and T. Nguyen, "A vortex Model of the Darrieus Turbine: An Analytical and Experimental Study", *Journal of Fluids Engineering*, Vol. 101, 1979, pp. 500–505.
- [5] F. N. Coton, D. Jiang, and R. A. M. Galbraith, "An Unsteady Prescribed Wake Model for Vertical Axis Wind Turbines", *Proceedings of the Institution of Mechanical Engineers Part A, Journal of Power and Energy*, Vol. 208, 1994, pp. 13–20.
- [6] M. O. L. Hansen, and D. N. Sørensen, "CFD Model for Vertical Axis Wind Turbine", *Wind Energy for the New Millennium—Proceedings of the European Wind Energy Conference*, Copenhagen, Denmark, 2–6 July 2001.
- [7] C. J. Simão Ferreira, H. Bijl, G. van Bussel, and G. van Kuik, "Simulating Dynamic Stall in a 2D VAWT: Modeling Strategy, Verification and Validation with Particle Image Velocimetry Data", *Journal of Physics. Conference Series*, Vol. 75, 2007, Paper 012023.
- [8] M. Raciti Castelli, A. Englaro, and E. Benini, "The Darrieus Wind Turbine: Proposal for a New Performance Prediction Model based on CFD", *Energy* 36, 2011, pp. 4919-4934.
- [9] K. Horiuchi, I. Ushiyama, and K. Seki, "Straight Wing Vertical Axis Wind Turbines: a Flow Analysis", *Wind Engineering*, Vol. 29, 2005, pp. 243–252.
- [10] A. Iida, K. Kato, and A. Mizuno, "Numerical Simulation of Unsteady Flow and Aerodynamic Performance of Vertical Axis Wind Turbines with LES", *16th Australasian Fluid Mechanics Conference*, Crown Plaza, Gold Coast, Australia, 2-7 December 2007.
- [11] R. Dominy, P. Lunt, A. Bickerdyke, and J. Dominy, "Self Starting Capability of a Darrieus Turbine", *Proceedings of the Institution of Mechanical Engineers Part A, Journal of Power and Energy*, Vol. 221, 2006, pp. 111–120.
- [12] B. Habtamu, and Y. Yingxua, "Numerical Simulation of Unsteady Flow to Show Self Starting of Vertical Axis Wind Turbine Using Fluent", *Journal of Applied Sciences*, Vol. 11, 2011, pp. 962–970.
- [13] B. Habtamu, and Y. Yingxua, "Effect of Camber Airfoil on Self Starting of Vertical Axis Wind Turbine", *Journal of Environmental Science and Technology*, Vol. 4, 2011, pp. 302–312.
- [14] V.T. Nguyen, C.C. Nguyen, T.H.H. Le, "Optimal aerodynamic design and generator matching for VAWT of 1kW using DMST method", *Journal of Transportation Science and Technology*, ISSN: 1859-4263, Vol. 7&8 - 9/2013, pp. 179-184.
- [15] http://www.ginlong.com/download/200908/GL-PMG-1000_Specification_Sheet.pdf.
- [16] K. E. Johnson, and L. J. Fingersh "Methods for Increasing Region 2 Power Capture on a Variable Speed HAWT", *Proceedings of the 23rd ASME Wind Energy Symposium*, 2004, pp. 103–113.
- [17] A. Kazumasa, M. Baku, Nagai, and N. R. Jitendro, "Design of a 3 kW Wind Turbine Generator with Thin Airfoil Blades", *Experimental Thermal and Fluid Science*, Vol. 32, 2008, pp. 1723–1730.

Biography



Chi-Cong Nguyen (1978, Vietnam) PhD in Fluid Mechanics, Heat Transfer and Combustions (2006, Aerodynamic Instability of Solid Rocket Motor) - Ecole Nationale Supérieure de Mécanique et d'Aérotechnique (ENSMA), Université de Poitiers, France.

Senior Lecturer and Researcher at Department of Aerospace Engineering, Ho Chi Minh City University of Technology, Vietnam. Research experience: Wind Engineering, Aero-elasticity, Aerodynamics, Turbulence, Multiphases flow, Heat transfer, Computational Fluid Dynamics. Head of the Department of Aerospace Engineering at Ho Chi Minh City University of Technology. About 5 publications in scientific and professional papers and about 10 papers on conference proceedings.



Thi-Hong-Hieu Le (1977, Vietnam) Ph.D in Aerodynamics and Fluids Mechanics (2005) – University of Poitiers, Aerodynamics Research Center, France. Senior Lecturer and Researcher at Department of Aerospace Engineering, Ho Chi Minh City University of Technology, Vietnam since 2007. Research interests: Computational Fluid Dynamics,

Flapping wing mechanisms, Experimental and numerical study on Aerodynamics of Vertical Axis Wind Turbines. Deputy-head of Department of Aerospace Engineering. About 10 journal and conference papers.



Phat-Tai Tran (1990, Vietnam) Engineer in Aerospace Engineering (2013, Aerodynamic performance of vertical axis wind turbine) - Ho Chi Minh City University of Technology, Vietnam. Research and work experience: Wind Engineering, Information Technology, CFD.